Controlling arbitrary observables in correlated many-body systems

Gerard McCaul [1,*] Christopher Orthodoxou,[2,†] Kurt Jacobs [3,4,5] George H. Booth,[2,‡] and Denys I. Bondar [1,§]

[1]*Department of Physics, Tulane University, New Orleans, Louisiana 70118, USA*

[2]*Department of Physics, King's College London, Strand, London WC2R 2LS, United Kingdom*

[3]*U.S. Army Research Laboratory, Computational and Information Sciences Directorate, Adelphi, Maryland 20783, USA*

[4]*Department of Physics, University of Massachusetts at Boston, Boston, Massachusetts 02125, USA*

[5]*Hearne Institute for Theoretical Physics, Louisiana State University, Baton Rouge, Louisiana 70803, USA*

Here we present an expanded analysis of a model for the manipulation and control of observables in a strongly correlated, many-body system, which was first presented by McCaul *et al.* [G. McCaul *et al.*, Phys. Rev. Lett. **124**, 183201 (2020)]. A field-free, nonlinear equation of motion for controlling the expectation value of an essentially arbitrary observable is derived, together with rigorous constraints that determine the limits of controllability. We show that these constraints arise from the physically reasonable assumptions that the system will undergo unitary time evolution, and has enough degrees of freedom for the electrons to be mobile. Furthermore, we give examples of multiple solutions to generating target observable trajectories when the constraints are violated. Ehrenfest theorems are used to further refine the model and provide a check on the validity of numerical simulations. Finally, the experimental feasibility of implementing the control fields generated by this model is discussed.

I. INTRODUCTION

The study of the control of quantum systems has a rich history [1], encompassing a diverse array of strategies. This includes optimal control [2,3] where a system is steered to a final target state using iterative optimization [4–6], possibly under additional constraints [7,8]. Local control [9] forgoes this iterative procedure and chooses a control field based on a system response such that the expectation of a target operator is monotonically increased [10]. This has been applied both to counteracting decoherence in molecular systems [11] and control of magnetic nanoparticles [12]. Separate from this is *tracking control* [13–18], where a physical system is evolved in such a way that a chosen observable conforms to (or "tracks") a preselected trajectory. This procedure can be thought of as local control applied to a time-dependent target state.

Examples of tracking control abound, with applications as diverse as singularity-free tracking of molecular rotors [14], optimizing dynamics within the density matrix renormalization group [3,15], and spectral dynamical mimicry, where a shaped pulse is used to induce an arbitrary desired spectrum in an atomic system [16]. While tracking control is far more computationally efficient than optimal control (as it requires one to simulate only a single evolution of the system, rather than iteratively exploring the space of control fields), if one attempts to track a trajectory that is inconsistent with the system's physically allowed dynamics, singularities in the control field emerge and tracking breaks down. In a recent paper [19],

a model for the tracking control of a many-electron system was presented without derivation. One of this model's main advantages was the ability to explicitly identify when control field singularities could occur. Here, we expand greatly upon that work, in three principal directions.

First, the tracking model used in Ref. [19] is explored in Sec. II. Starting from general considerations of an *N*-electron Hamiltonian, a comprehensive derivation of the tracking equation is presented. Additionally, in Sec. III, we derive, for a finite-dimensional system, the precise constraints on tracking necessary both to avoid singularities and to guarantee a unique evolution. A simple example where these constraints are not obeyed and multiple solutions for the tracking field are possible is also provided.

Given that in tracking control one recovers the expected observable trajectory by design, a method of verifying that the numerical calculations are physically valid is vital. To this end, we detail in Sec. IV the application of an Ehrenfest theorem to the model as a way both to verify simulations and to remove nonphysical discontinuities from the control fields.

In Sec. V, we examine the tracking control strategy that arises when the system model is continuous and the consequences of this for the properties of the control scheme. Finally, with the purpose of further exploring the experimental requirements of the control protocol, we examine in Sec. VI the performance of the control fields detailed in Ref. [19] when the calculated fields are fitted to an experimentally feasible set of parameters. We close in Sec. VII with a discussion of the results and questions for future work.

II. TRACKING MODEL

A. Background

Our goal is to implement a tracking control [17] model for a general *N*-electron system subjected to a laser pulse

* gmccaul@tulane.edu

† christopher.orthodoxou@kcl.ac.uk

‡ george.booth@kcl.ac.uk

§ dbondar@tulane.edu

described by the Hamiltonian (using atomic units) [20]

$$\hat{H} = \sum_{\sigma} \int \frac{dx}{2} \hat{\psi}^{\dagger}(x)[i\partial_x - A(t)]^2 \hat{\psi}(x)$$
$$+ \sum_{\sigma\sigma'} \int \frac{dxdx'}{2} \hat{\psi}^{\dagger}_{\sigma'}(x')\hat{\psi}^{\dagger}_{\sigma}(x)U(x - x')\hat{\psi}_{\sigma}(x)\hat{\psi}_{\sigma'}(x'),$$
(1)

where $A(t)$ is the field vector potential, $U(x - x')$ is the two-body interaction potential, and $\hat{\psi}_{\sigma}(x)$ are the standard fermionic field operators satisfying $\{\hat{\psi}^{\dagger}_{\sigma'}(x'), \hat{\psi}_{\sigma}(x)\} = \delta_{\sigma\sigma'}\delta(x - x')$. Ultimately, we wish to calculate the control field $A_T(t)$, such that the trajectory of an expectation $\langle \hat{O}(t) \rangle$ follows some desired function $O_T(t)$ [13–16]. For the sake of specificity, here we derive the control field $A_T(t)$ necessary to control the current expectation, but emphasize that an expression can be derived for an arbitrary expectation using the technique described in Sec. II C. We first reexpress the model in an explicitly self-adjoint form using

$$\hat{\psi}^{\dagger}(x)[i\partial_x - A(t)]^2 \hat{\psi}(x)$$
$$= \partial_x[e^{iA(t)x}\hat{\psi}_{\sigma}(x)]^{\dagger} \partial_x[e^{iA(t)x}\hat{\psi}_{\sigma}(x)]. \quad (2)$$

In this form, one may straightforwardly construct a continuity equation for the density operator $\hat{\rho}(x) = \hat{\psi}^{\dagger}(x)\hat{\psi}(x)$:

$$\frac{d}{dt}\hat{\rho}(x) = i[\hat{H}, \hat{\rho}(x)] = -\partial_x \hat{J}(x), \quad (3)$$

which defines the current operator $\hat{J}(x)$,

$$\hat{J}(x) = \frac{1}{2i}[\hat{\psi}^{\dagger}(x)\partial_x\hat{\psi}(x) - \partial_x\hat{\psi}^{\dagger}(x)\hat{\psi}(x)] + A(t)\hat{\psi}^{\dagger}(x)\hat{\psi}(x).$$
(4)

The current expectation is obtained from this expression by taking expectations and integrating over space, i.e., $\int dx \langle \hat{J}(x) \rangle = J(t)$. Noting that $N = \langle \int \hat{\rho}(x)dx \rangle$ is a conserved quantity, one may straightforwardly invert Eq. (4) to obtain the $A_T(t)$ that corresponds to $\int dx \langle \hat{J}(x) \rangle = J_T(t)$:

$$A_T(t) = \frac{i}{2N} \int dx \langle \hat{\psi}^{\dagger}(x)\partial_x\hat{\psi}(x) - \partial_x\hat{\psi}^{\dagger}(x)\hat{\psi}(x) \rangle(t) + \frac{J_T(t)}{N}.$$
(5)

For systems with bosonic statistics, it is easy to show that the control field equation is almost identical, but the definition of the current operator picks up a negative sign, $\hat{J}(x) \to -\hat{J}(x)$.

B. Tracking control in a discrete model

While the equation for the tracking control field will, in principle, describe tracking for an N-electron system, in this paper we will provide a concrete illustration of its use with a lattice model. To do so, we first discretize the model Hamiltonian, using a as the lattice constant such that $x = ja$ and $x' = ka$,

$$\int dx \to \sum_r a \implies \delta(x - x') \to \frac{\delta_{jk}}{a}, \quad (6)$$

$$\hat{\psi}_{\sigma}(x) \to \frac{\hat{c}_{j\sigma}}{\sqrt{a}} \implies \{\hat{c}^{\dagger}_{j\sigma}, \hat{c}_{k\sigma'}\} = \delta_{jk}\delta_{\sigma\sigma'}, \quad (7)$$

$$\partial_x g(x) \to [g_{j+1} - g_j]/a. \quad (8)$$
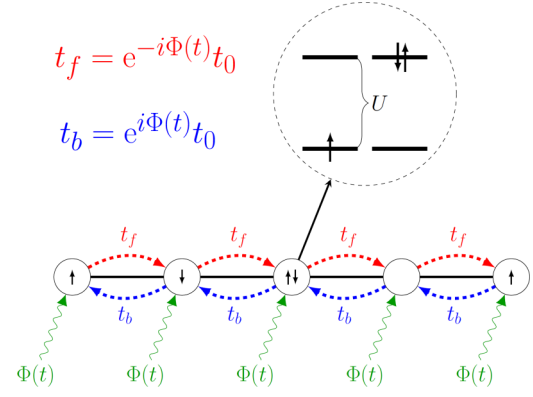
FIG. 1. Schematic representation of the Fermi-Hubbard model. Electrons hop between sites with an on-site repulsion of U, and a Hermitian hopping amplitude scaled by the applied field $\Phi(t)$.

After discretization and assuming periodic boundary conditions, the Hamiltonian takes the form

$$\hat{H} = - \sum_{j,\sigma} \frac{1}{2a^2} \left(e^{-i\Phi(t)}\hat{c}^{\dagger}_{j+1\sigma}\hat{c}_{j\sigma} + e^{i\Phi(t)}\hat{c}^{\dagger}_{j\sigma}\hat{c}_{j+1,\sigma} \right)$$
$$+ \sum_{j,\sigma} \frac{1}{a^2}\hat{c}^{\dagger}_{j\sigma}\hat{c}_{j\sigma} + \sum_{j,k,\sigma,\sigma'} U_{j-k}\hat{c}^{\dagger}_{k\sigma'}\hat{c}^{\dagger}_{k\sigma}\hat{c}_{j\sigma}\hat{c}_{j\sigma'}, \quad (9)$$

where we have set $\Phi(t) = aA(t)$. From this discretized Hamiltonian, one is able to derive a continuity equation for $\hat{\rho}_j = \sum_{\sigma} \hat{c}^{\dagger}_{j\sigma}\hat{c}_{j\sigma}$,

$$\frac{d\hat{\rho}_j}{dt} = \frac{1}{a}(\hat{J}_j - \hat{J}_{j-1}), \quad (10)$$

$$\hat{J}_j = -i\frac{1}{a}\sum_{\sigma} \left(e^{-i\Phi(t)}\hat{c}^{\dagger}_{j\sigma}\hat{c}_{j+1\sigma} - \text{H.c.} \right). \quad (11)$$

This continuity equation defines the current operator $\hat{J} = \sum_j \hat{J}_j$ and has the important property of being composed only from the kinetic part of the Hamiltonian. This means the current operator is not explicitly dependent on the form of the interaction U_{j-k}. As a result of this property, the construction of a method to track the expectation of the current operator does not depend on the specific form of the Hamiltonian's interparticle interactions. For this reason, we will restrict our derivation to a specific Hamiltonian, but emphasize that the results may be applied to any model with the form of Eq. (1).

From this point forward, we will use the one-dimensional (1D) Fermi-Hubbard model [21] (see Fig. 1 for a schematic representation) as a concrete example of the tracking strategy. This model has the Hamiltonian

$$\hat{H}(t) = - t_0 \sum_{j,\sigma} \left(e^{-i\Phi(t)}\hat{c}^{\dagger}_{j\sigma}\hat{c}_{j+1\sigma} + e^{i\Phi(t)}\hat{c}^{\dagger}_{j+1\sigma}\hat{c}_{j\sigma} \right)$$
$$+ U \sum_j \hat{c}^{\dagger}_{j\uparrow}\hat{c}_{j\uparrow}\hat{c}^{\dagger}_{j\downarrow}\hat{c}_{j\downarrow}. \quad (12)$$

As in the continuum case, we wish to find the vector potential that will produce a specified current $J_T(t) = \langle \hat{J} \rangle$. To do so, we

take the current expectation,

$$\hat{J} = -iat_0 \sum_{j,\sigma} \left(e^{-i\Phi(t)} \hat{c}_{j\sigma}^\dagger \hat{c}_{j+1\sigma} - \text{H.c.} \right), \qquad (13)$$

and rearrange for Φ, expressing the nearest-neighbor expectation in a polar form,

$$\langle \psi(t) | \sum_{j,\sigma} \hat{c}_{j\sigma}^\dagger \hat{c}_{j+1\sigma} | \psi(t) \rangle = R(\psi) e^{i\theta(\psi)}. \qquad (14)$$

In both Eq. (14) and later expressions, the argument ψ indicates that the expression is dependent on a functional of $|\psi\rangle \equiv |\psi(t)\rangle$. Equation (14) can be used in conjunction with Eq. (13) to yield

$$
\begin{aligned}
J(t) &= -iat_0 R(\psi) \left(e^{-i[\Phi(t)-\theta(t)]} - e^{i[\Phi(t)-\theta(\psi)]} \right) \\
&= -2at_0 R(\psi) \sin[\Phi(t) - \theta(\psi)].
\end{aligned} \qquad (15)
$$

An important caveat that should be noted here is that if one were to apply a time-dependent rotation to the system, the current expectation would no longer depend explicitly on $\Phi(t)$ [22], but instead there would remain an implicit dependence through the state of the system $|\psi\rangle$. This is important, as in order to define a control field which reproduces a tracking current $J_T(t)$, we invert Eq. (15). From this inversion, we obtain the tracking control field $\Phi_T(t, \psi)$, which takes the desired current expectation as a parameter,

$$\Phi_T(t, \psi) = \arcsin\left[-X(t, \psi)\right] + \theta(\psi), \qquad (16)$$

in which we have defined

$$X(t, \psi) = \frac{J_T(t)}{2at_0 R(\psi)}. \qquad (17)$$

From Eq. (16), it is possible to eliminate the control field entirely from the model Hamiltonian using the equality

$$e^{\pm i\Phi_T(t, \psi)} = e^{\pm i\theta(\psi)} \left[\sqrt{1 - X^2(t, \psi)} \mp iX(t, \psi) \right], \qquad (18)$$

where the above equality is obtained via Euler's equation and $\cos[\arcsin(x)] = \sqrt{1 - x^2}$. From this, we are able to define the "tracking Hamiltonian" $\hat{H}_T(J_T(t), \psi)$, which takes the target current $J_T(t)$ as a parameter,

$$
\begin{aligned}
\hat{H}_T(J_T(t), \psi) &= \sum_{\sigma,j} [P_+ e^{-i\theta(\psi)} \hat{c}_{j\sigma}^\dagger \hat{c}_{j+1\sigma} + \text{H.c.}] \\
&\quad + U \sum_j \hat{c}_{j\uparrow}^\dagger \hat{c}_{j\uparrow} \hat{c}_{j\downarrow}^\dagger \hat{c}_{j\downarrow},
\end{aligned} \qquad (19)
$$

$$P_\pm = -t_0 [\sqrt{1 - X^2(t, \psi)} \pm iX(t, \psi)]. \qquad (20)$$

This leads to a field-free, nonlinear evolution for the wave function given by

$$i \frac{d|\psi\rangle}{dt} = \hat{H}_T(J_T(t), \psi) |\psi\rangle, \qquad (21)$$

which is equivalent to evolving the system with the original Hamiltonian given in Eq. (12) and the usual Schrödinger equation $i\frac{d|\psi\rangle}{dt} = \hat{H}(t)|\psi\rangle$, under the additional constraint that $\Phi(t)$ is chosen such that $\langle \hat{J}(t) \rangle = J_T(t)$. After solving Eq. (21), it is also possible to recover the tracking field $\Phi_T(t)$ via Eq. (16).
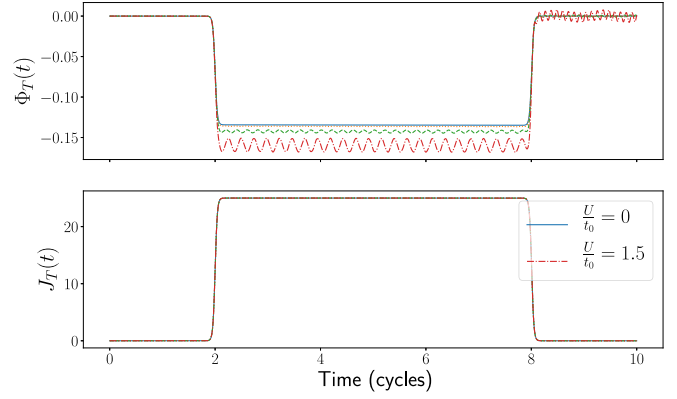
FIG. 2. Induced switching currents via tracking such that the current models Eq. (22). Electron-electron interactions at strengths of $U = [0, 0.5, 1, 1.5]t_0$ are shown. The upper panel shows that the necessary control field needed to reproduce this current is sensitive to the correlation strength.

As a first test for the tracking strategy, we use it to dynamically manipulate the current of a system so that it changes abruptly from zero to nonzero and back, which can therefore be used as a current "switch." Forcing $J_T(t)$ to track an arbitrary function is possible, provided the tracking conditions are obeyed (see Sec. III). We therefore assign the target current $J_T(t)$ to a boxlike switch function,

$$J_T(t) = \frac{1}{4(1 + e^{-2(t-T/5)})} - \frac{1}{4(1 + e^{-2(t-4T/5)})}. \qquad (22)$$

In Fig. 2, we show the result of applying the tracking algorithm, along with the tracking phase $\Phi_T(t)$ necessary to produce $J_T(t)$ at several interaction strengths. While the target current can be tracked at all selected model parameters, increasing the on-site repulsion results in compensatory oscillations within the control phase $\Phi_T(t)$. This reflects the increasing nonlinearity in the equation of motion as one increases the on-site repulsion.

C. Tracking arbitrary observables

Finally, we extend the derivation for tracking current to an arbitrary observable $\hat{O} = \hat{O}^\dagger$, whose expectation $O(t) = \langle \hat{O} \rangle$ is not a function of Φ. In this case, the time derivative is

$$
\begin{aligned}
\frac{dO(t)}{dt} &= it_0 \sum_{j,\sigma} (e^{-i\Phi(t)} \langle [\hat{c}_{j\sigma}^\dagger \hat{c}_{j+1,\sigma}, \hat{O}] \rangle + \text{H.c.}) \\
&\quad - iU \sum_j \langle [\hat{c}_{j\uparrow}^\dagger \hat{c}_{j\uparrow} \hat{c}_{j\downarrow}^\dagger \hat{c}_{j\downarrow}, \hat{O}] \rangle.
\end{aligned} \qquad (23)
$$

From this evolution, we assign

$$\sum_{j,\sigma} \langle [\hat{c}_{j\sigma}^\dagger \hat{c}_{j+1,\sigma}, \hat{O}] \rangle = R_O e^{i\theta_O}, \qquad (24)$$

$$B = -iU \sum_j \langle [\hat{c}_{j\uparrow}^\dagger \hat{c}_{j\uparrow} \hat{c}_{j\downarrow}^\dagger \hat{c}_{j\downarrow}, \hat{O}] \rangle. \qquad (25)$$

With this substitution, we obtain an expression for the derivative of the observable in terms of the control field,

$$\frac{dO(t)}{dt} = -2t_0 R_O \sin(\Phi - \theta_O) + B. \qquad (26)$$

This can be inverted to obtain the tracking control field for an arbitrary observable,

$$\Phi_O = \arcsin\left(\frac{B - \frac{dO}{dt}}{2t_0 R_O}\right) + \theta_O. \tag{27}$$

From this, a tracking Hamiltonian and constraint can be derived using the methods presented previously. The theoretical considerations in the rest of this paper may be applied to tracking an arbitrary variable, but in the interests of clarity we shall restrict our attention to tracking of the current expectation using Eq. (19).

III. TRACKING CONSTRAINTS

In this section, we prove the following statement:

For a finite system, if the wave function $|\psi\rangle \equiv |\psi(t)\rangle$ solves Eq. (21) and satisfies the constraints

$$|X(t, \psi)| < 1 - \epsilon_1, \tag{28}$$

$$R(\psi) > \epsilon_2, \tag{29}$$

where ϵ_1, ϵ_2 are any positive constants, then $|\psi\rangle$ is a unique solution of Eq. (21) and therefore, by Eq. (16), $\Phi_T(t)$ is a unique field which solves the current tracking problem.

Both of the constraints given by Eqs. (28) and (29) are necessary conditions for $\hat{H}_T(J_T(t), \psi)$ to be *Lipschitz continuous* (LC) over $|\psi\rangle$ [23]. In this case, the Picard-Lindelöf theorem guarantees $|\psi\rangle$ has a unique solution depending on its initial value when being evolved by the tracking Hamiltonian [24].

In Sec. III A, we formally show that under the constraints given by Eqs. (28) and (29), the tracking Hamiltonian is LC, while in Sec. III B, we provide a physical motivation for these constraints. Finally, in Sec. III C, we provide a simple example where the derived constraints do not hold and multiple solutions for the tracking field are possible.

A. Proving Lipschitz continuity

We define the L_2 norm $\||\psi\rangle\|_2 = \sqrt{\langle\psi|\psi\rangle}$ and spectral norm [25],

$$\|\hat{A}\|_{\mathcal{L}} = \sup_{\langle\psi|\psi\rangle=1} \|\hat{A}|\psi\rangle\|_2. \tag{30}$$

These norms obey a submultiplicative property [26],

$$\|\hat{A}|\psi\rangle\|_2 \leqslant \|\hat{A}\|_{\mathcal{L}} \||\psi\rangle\|_2, \tag{31}$$

which, when combined with the Cauchy-Schwarz inequality, yields

$$|\langle\phi|\hat{A}|\psi\rangle| \leqslant \||\phi\rangle\|_2 \|\hat{A}|\psi\rangle\|_2 \leqslant \||\phi\rangle\|_2 \|\hat{A}\|_{\mathcal{L}} \||\psi\rangle\|_2. \tag{32}$$

We now proceed to prove that for the set of wave functions which obeys Eqs.(28) and (29), the following inequality holds:

$$\|\hat{H}_T(J_T(t), \psi)|\psi\rangle - \hat{H}_T(J_T(t), \phi)|\phi\rangle\|_2 \leqslant L_H \||\psi\rangle - |\phi\rangle\|_2, \tag{33}$$

where L_H is some finite constant, and is the definition of LC for the function $\hat{H}_T(J_T(t), \psi)|\psi\rangle$. In order to prove this, it is convenient to establish some properties both for operators and functionals of $|\psi\rangle$.

First, in finite dimensions, all linear operators are bounded, which implies that they are also LC over the whole Hilbert space,

$$\|\hat{A}(|\psi\rangle - |\phi\rangle)\|_2 \leqslant \|\hat{A}\|_{\mathcal{L}} \||\psi\rangle - |\phi\rangle\|_2. \tag{34}$$

Additionally, the expectation of linear operators $\langle\psi|\hat{A}|\psi\rangle = A(\psi)$ is also LC on the space of wave functions ($\||\psi\rangle\|_2 = 1$). This is demonstrated by taking the identity

$$A(\psi) - A(\phi) = \langle\psi|\hat{A}|\psi\rangle - \langle\phi|\hat{A}|\phi\rangle$$
$$= \langle\psi|\hat{A}(|\psi\rangle - |\phi\rangle) - ((\langle\phi| - \langle\psi|)\hat{A}|\phi\rangle, \tag{35}$$

and applying the triangle inequality $|x + y| \leqslant |x| + |y|$ to its norm,

$$|A(\psi) - A(\phi)| \leqslant 2\|\hat{A}\|_{\mathcal{L}} \||\psi\rangle - |\phi\rangle\|_2. \tag{36}$$

More generally, an arbitrary functional of $|\psi\rangle$, $f : |\psi\rangle \to \mathbb{C}$ is LC over $|\psi\rangle$ if, for all $|\psi\rangle, |\phi\rangle$ in its domain, it satisfies the inequality

$$|f(\psi) - f(\phi)| \leqslant L_f \||\psi\rangle - |\phi\rangle\|_2, \tag{37}$$

where L_f is some finite constant. Taking two functionals $f(\psi), g(\psi)$, which are LC over $|\psi\rangle$ with Lipschitz constants L_f and L_g, the norm of their product $h(\psi) = f(\psi)g(\psi)$ is

$$|h(\psi) - h(\phi)| = |[f(\psi) - f(\phi)]g(\psi) + f(\phi)[g(\psi) - g(\phi)]|$$
$$\leqslant |f(\psi) - f(\phi)||g(\psi)| + |f(\phi)||g(\psi) - g(\phi)|$$
$$\leqslant [L_f|g(\psi)| + L_g|f(\phi)|]\||\psi\rangle - |\phi\rangle\|_2. \tag{38}$$

This means that if the functionals $f(\psi), g(\psi)$ are LC *and* bounded over the domain of ψ, then their product is also LC. In the case of a product between an operator and an LC functional, $f(\psi)\hat{A}$, a similar result to Eq. (38) is obtained:

$$\|f(\psi)\hat{A}|\psi\rangle - f(\phi)\hat{A}|\phi\rangle\|_2$$
$$\leqslant \|\hat{A}\|_{\mathcal{L}}[L_f + |f(\psi)|]\||\psi\rangle - |\phi\rangle\|_2, \tag{39}$$

i.e., if $f(\psi)$ is bounded and LC, then $f(\psi)\hat{A}$ is also LC. Lastly, sums of any LC operators or functionals will themselves be LC by the triangle inequality.

Equipped with these properties, the most direct route to proving Eq. (33) is to prove that each of the constituent components of Eq. (19) is both LC and bounded, which by Eqs. (38) and (39) and the triangle inequality is sufficient to prove that the tracking Hamiltonian is itself LC in ψ.

The relevant parts of the Hamiltonian for which Lipschitz continuity over $|\psi\rangle$ and boundedness must be demonstrated are $e^{i\theta(\psi)}$ and $P_\pm$. To prove the former is LC, we first consider the nearest-neighbor expectation, using $\sum_{j,\sigma} \hat{c}_{j\sigma}^\dagger \hat{c}_{j+1\sigma} = \hat{K}$,

$$\langle\psi|\hat{K}|\psi\rangle = K(\psi) = R(\psi)e^{i\theta(\psi)}. \tag{40}$$

This expectation is LC by Eq. (36), and bounded due to Eq. (32) and the normalization of the wave functions. Combining this result with the reverse triangle inequality $||x| - |y|| \leqslant |x - y|$ further demonstrates that $R(\psi) = |K(\psi)|$ is also LC and bounded. The final step in order to show $e^{i\theta(\psi)}$ is itself LC is to establish that $R^{-1}(\psi)$ is LC under Eqs. (28) and (29). This is easily established by

$$|R^{-1}(\psi) - R^{-1}(\phi)| = \frac{1}{R(\psi)R(\phi)}|R(\psi) - R(\phi)|$$

$$\leqslant \frac{1}{\epsilon_2^2}\|\hat{K}\|_{\mathcal{L}}\||\psi\rangle - |\phi\rangle\|_2, \qquad (41)$$

where in the second inequality we have utilized Eq. (29). By Eq. (38), we therefore establish $e^{i\theta(\psi)} = \frac{K(\psi)}{R(\psi)}$ is LC and is bounded by definition.

The final term to tackle is $P_\pm$. Since this is the only term that involves our target $J_T(t)$, we work directly in the variable $x = X(t, \psi)$. The function $f(x) = x$ is itself trivially LC and bounded over this domain where Eq. (28) is satisfied. It therefore only remains to check the Lipschitz continuity of $f(x) = \sqrt{1 - x^2}$. Since this function is differentiable on the interval $I = [-(1 - \epsilon_1), 1 - \epsilon_1]$ which satisfies Eq. (28), by the mean value theorem [27] the function is LC if $|f'(x)| \leqslant M$ for all $x \in I$ and M is finite. It is easy to show that

$$M = \max_{x \in I}|f'(x)| = \frac{1 - \epsilon_1}{2\sqrt{2\epsilon_1 - \epsilon_1^2}}, \qquad (42)$$

and therefore $P_\pm$ is LC and bounded provided $\epsilon_1 \neq 0$ and < 1. Note that the presence of $\epsilon_{1/2}$ in the tracking conditions is necessary to exclude the neighborhood around which L_H becomes unbounded. As a result, we establish that under the conditions of Eqs. (28) and (29), each of the components of the tracking Hamiltonian is LC and bounded, meaning that the Hamiltonian is itself LC. From this continuity, it follows that the Picard-Lindelöf theorem is obeyed and $|\psi\rangle$ has a unique solution depending on its initial value. It is interesting to note that this result, derived from the analysis of the continuous formulation (19), stands in sharp contrast to some discretized approaches to tracking problems, in which multiple solutions are possible [28].

B. Physical motivation

It is reasonable to ask whether the constraints imposed upon ψ are well justified, and here we provide physical motivation for them. First, the condition $|X(t, \psi)| < 1 - \epsilon_1$ is easily justified by noting that if this is violated, $P_+^\dagger \neq P_-$ and the tracking Hamiltonian in Eq. (19) is no longer Hermitian. This constraint therefore corresponds to a restriction on the currents that can be produced in a physical system to ensure that the state undergoes appropriate unitary time evolution.

The restriction imposed by Eq. (29) is somewhat more general as it does not make reference to the current being tracked. Nevertheless, we shall demonstrate here that it is reasonable to expect this property in physical systems. We first consider $\hat{K}$ in a diagonal basis, using the transformation $\hat{c}_{j\sigma} = \sum_k e^{i\omega_k j}\tilde{c}_{k\sigma}$, where $\omega_k = \frac{2\pi k}{L}$, and L is the number of
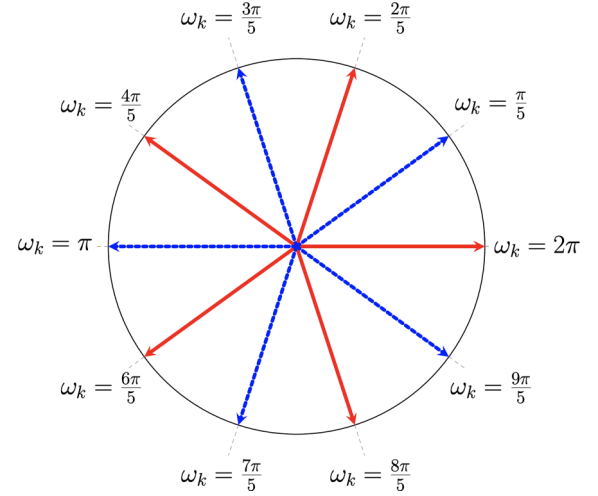
FIG. 3. An example of the contributions to $K(\psi)$ for $L = 10$ sites at half filling. In this example, the occupied states for one-spin species (dashed blue) have been chosen so that they are in antiphase with the other species (red), and therefore $K(\psi) = 0$.

sites. The nearest-neighbor expectation then assumes the form

$$K(\psi) = \sum_{k,\sigma}[\cos(\omega_k) + i\sin(\omega_k)]\langle\psi|\tilde{c}_{k\sigma}^\dagger\tilde{c}_{k\sigma}|\psi\rangle. \qquad (43)$$

In the diagonal space, we immediately see that every occupied state in momentum space contributes components with equal magnitude, but which differ by a phase. For an even number of particles (as is always the case at half filling), it is mathematically very easy to construct an arbitrary wave function such that each occupied state's contribution is in antiphase with another, making $K(\psi) = 0$ and violating the tracking constraint. A simple example of this is shown in Fig. 3.

While it is possible to construct a wave function which violates Eq. (29), the question is whether such a wave function is truly physical. To answer this, we consider Eq. (12) in the tight-binding limit ($\frac{U}{t_0} = 0$). In the diagonalized basis, this Hamiltonian is [29,30]

$$\hat{H}(t) = -2t_0\sum_{k,\sigma}\cos[\omega_k - \Phi(t)]\tilde{c}_{k\sigma}^\dagger\tilde{c}_{k\sigma}. \qquad (44)$$

Notice that this shares a common eigenbasis with the nearest-neighbor expectation. While the tracking strategy is insensitive to the initial state, we consider here a system that begins in the ground state $|\psi_g\rangle$, minimizing the system energy. Since the Hamiltonian is diagonal in the occupation number basis, the ground state will be a pure state [31] in this representation, and has energy

$$\langle\psi_g|\hat{H}(0)|\psi_g\rangle = -2t_0\sum_{k,\sigma}\cos(\omega_k)\delta(k,\sigma) = E_g, \qquad (45)$$

where $\delta(k,\sigma) = \langle\psi_g|\tilde{c}_{k\sigma}^\dagger\tilde{c}_{k\sigma}|\psi_g\rangle$ is 1 if the relevant mode is occupied in the ground state, and zero otherwise.

Clearly, the occupation numbers of the ground state will be such that Eq. (45) is *minimized*. If one has $N = \sum_\sigma N_\sigma$ particles on an L-site lattice, each spin species' contribution to the ground-state energy will consist of the N_σ momentum modes closest to $\omega_k = 0$. From this counting argument, it is

possible to give an analytic expression for $E_g = \sum_\sigma E_\sigma$,

$$-\frac{E_\sigma}{2t_0} = \begin{cases} 1 + 2\sum_{k=1}^{\frac{N_\sigma}{2}-1} \cos\omega_k + \cos\frac{\pi N_\sigma}{L} & \text{if } N_\sigma > 0 \text{ is even,} \\ 1 + 2\sum_{k=1}^{\frac{N_\sigma-1}{2}} \cos\omega_k & \text{if } N_\sigma \text{ is odd.} \end{cases}$$
(46)

It is easy to see from this analytic expression that the only cases for which E_g is zero are either the vacuum or when every mode of both spin species is occupied, and the system dynamics are completely frozen.

Having established that E_g is nonzero in all but the most trivial of circumstances, we now substitute it into the nearest-neighbor expectation to obtain $K(\psi_g)$,

$$K(\psi_g) = \langle\psi_g| \sum_{j,\sigma} \hat{c}_{j\sigma}^\dagger \hat{c}_{j+1\sigma} |\psi_g\rangle = -\frac{E_g}{2t_0} + \lambda, \qquad (47)$$

$$\lambda = i\sum_k \delta(k,\sigma)\sin(\omega_k), \qquad (48)$$

which means that for the ground state, $K(\psi_g)$ has a nonzero real part and $R(\psi_g)$ *must* be nonzero. Furthermore, since the Hamiltonian and nearest-neighbor operators commute at all times in the diagonal basis, the value of $R(\psi)$ is time independent and therefore nonzero for all ψ that can be evolved from the ground state.

In a system with nonzero U, we can consider only the kinetic term, which has the form

$$\hat{H}_K = -t_0 \sum_{j,\sigma} (\hat{c}_{j\sigma}^\dagger \hat{c}_{j+1\sigma} + \hat{c}_{j+1\sigma}^\dagger \hat{c}_{j\sigma}). \qquad (49)$$

In this case, provided $\langle\psi|\hat{H}_K|\psi\rangle \neq 0$, an analogous argument can be made to justify Eq. (29). For this reason, we can consider that this constraint corresponds to the condition that there is some kinetic energy in the system, and the electrons have not been completely frozen (a natural precondition for observing *any* current).

We conclude this section with the observation that while, in principle, the derived constraints are highly nonlinear inequalities in $|\psi\rangle$, in practice, simulations confirm the expectation that even at high $\frac{U}{t_0}$, Eq. (29) is obeyed (see, e.g., Fig. 7). Furthermore, it is relatively easy to satisfy Eq. (28) via a heuristic scaling of the target to be tracked, as these constraints limit only the peak amplitude of current in the evolution, and otherwise allow for any function to be tracked when appropriately scaled. If one is concerned only with reproducing the shape of the target current, then using a scaled target $J_s(t) = kJ_T(t)$ such that $|J_s(t)| < 2at_0R(t)$ will allow tracking unproblematically. Alternately, if one treats the lattice constant a as a tunable parameter, this can always be set for the tracking system so as to satisfy $|X(t,\psi)| < 1 - \epsilon_2$.

Singularities in the control field are a common occurrence in tracking control, which often make a specified trajectory impossible to reproduce [14,17,32]. While singularities are present in the unconstrained model presented here, they are easily identified and avoided using the constraints derived above.
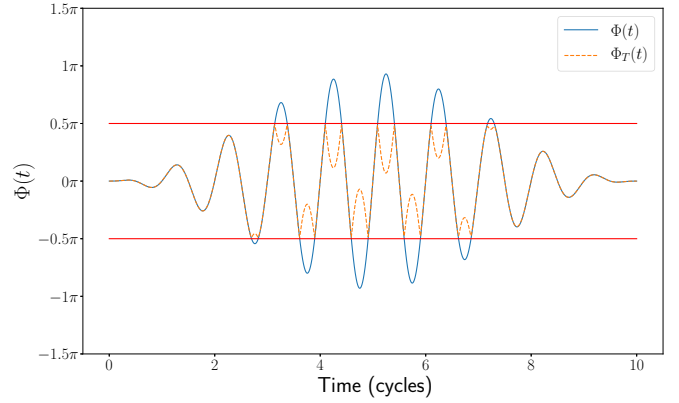
FIG. 4. Control fields driving a $U = 0$ system, each of which generates the same current. Here there are multiple solutions, $\Phi(t) \neq \Phi_T(t)$, due to the violation of Eq. (28) at $\Phi(t) = \pm\frac{\pi}{2}$.

C. Multiple solutions

We conclude this section with a demonstration that when the derived constraints of Eqs. (28) and (29) are not both satisfied, multiple solutions for $|\psi\rangle$ and hence $\Phi_T(t)$ are possible. To simplify the algebra, we consider a $U = 0$ system, where $\theta(\psi) = 0$ regardless of the field applied when evolving from the ground state.

Now consider a situation where one uses tracking simply to reproduce the current produced by some field $\Phi(t)$, i.e., $J_T(t) = J(t)$, and if the solution is unique, $\Phi_T = \Phi(t)$. Applying tracking to this situation, if

$$\Phi(0) = 0, \quad |\Phi(t)| < \frac{\pi}{2}, \qquad (50)$$

then the solution is unique and $\Phi_T(t) = \Phi(t)$.

If, however, there is a point where $|\Phi(t)| = \frac{\pi}{2}$, then $X(t,\psi) = 1$ and Eq. (28) is violated. If the control field is continuous, then any $\Phi(t)$ which does not obey Eq. (50) also violates Eq. (28). Figure 4 confirms this violation, where both control fields generate the same current [shown in Fig. 6(a)], but have different functional forms.

The multiplicity of the solutions shown can be understood physically in a simple manner. Reproducing the target current only requires that $\sin[\Phi(t)] = \sin[\Phi_T(t)]$, but identical dynamics requires $e^{\pm i\Phi(t)} = e^{\pm i\Phi_T(t)}$. The latter condition is much stricter, and only coincides with the tracking requirements when Eq. (50) is also obeyed. This phenomenon is illustrated in Fig. 5, where crossing the threshold produces two solutions that will track the target observable. It is therefore possible to generate tracking control fields which reproduce the target, but have quite different dynamics and, hence, multiple solutions for $|\psi\rangle$ and $\Phi_T(t)$.

We conclude this section with the observation that even in the case that $|\psi\rangle$ is unique, the tracking field $\Phi_T(t)$ defined in Eq. (16) will only be unique modulo 2π. This constitutes a nonuniqueness in the tracking field *at each time step*. Fortunately, one is able to appeal to another physical principle to eliminate this nonuniqueness, namely, that the system obey an *Ehrenfest theorem* for current.
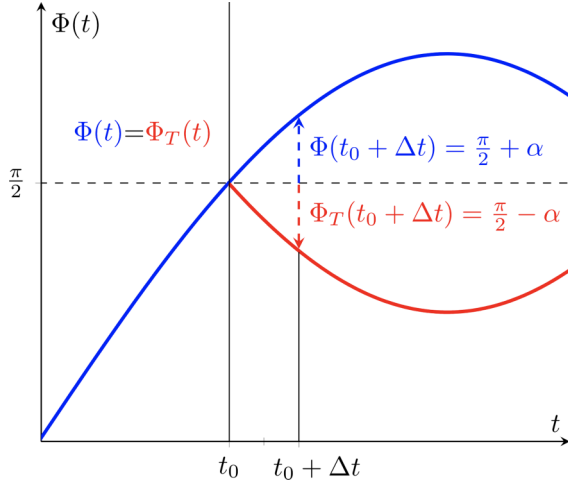
FIG. 5. When reproducing a current, while $|\Phi(t)| < \frac{\pi}{2}$, the solution is unique and $\Phi(t) = \Phi_T(t)$. If, however, at some time t_0, $\Phi(t_0) < \frac{\pi}{2}$ and at the next time step $\Phi(t_0 + \Delta t) = \frac{\pi}{2} + \alpha$, then the solution $\Phi_T(t_0 + \Delta t) = \frac{\pi}{2} - \alpha$ will generate the same current, but $e^{\pm i\Phi_T(t_0 + \Delta t)} = e^{\pm 2i\alpha}e^{\pm i\Phi(t_0 + \Delta t)}$, breaking the dynamical symmetry between the two systems.

IV. EHRENFEST THEOREMS

We now turn our attention to the question of verification of numerical simulations. Given that the tracking strategy will, by definition, reproduce the trajectory one desires, it is important to have an independent check that tracking has been achieved via a physical evolution rather than numerical aberrations. A particularly sensitive test of the physicality of a numerical simulation is checking that expectations obey the relevant Ehrenfest theorems (see, e.g., Ref. [15]). These relate derivatives of a given expectation to other expectations. In the Hubbard model, there is an Ehrenfest theorem for $J(t)$, namely,

$$
\frac{dJ(t)}{dt} = eat_0 e^{-i\Phi(t)} \sum_{j,\sigma} \left(\langle [\hat{H}(t), c_{j\sigma}^{\dagger} c_{j+1\sigma}] \rangle \right.
$$
$$
\left. - \frac{d\Phi(t)}{dt} \langle c_{j,\sigma}^{\dagger} c_{j+1,\sigma} \rangle \right) + \text{H.c.}, \tag{51}
$$

which must be respected if the evolution is physical.

An important feature of the tracking Hamiltonian is that although the tracked variable will be reproduced by construction, there is no guarantee that any other observables will be tracked. This means that we only know *a priori* the left-hand side of Eq. (51), which will correspond by construction to $\frac{dJ_t}{dt}$, and can therefore verify that a simulation respects physical principles by checking that the independent expectations from the right-hand side of Eq. (51) are correct. To do so, we assign to the commutator in the first term of (51) the following shorthand:

$$
\frac{1}{U} \sum_{j,\sigma} \langle [\hat{H}(t), c_{j\sigma}^{\dagger} c_{j+1\sigma}] \rangle = C(\psi) e^{i\kappa(\psi)}, \tag{52}
$$

from which we obtain an analytic expression for the current derivative in terms of the independent expectations defined by
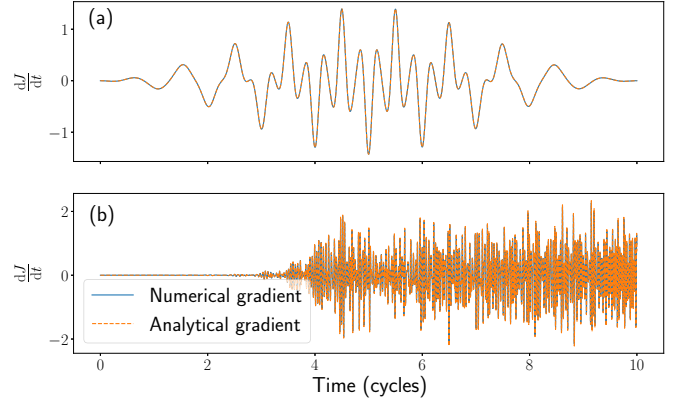
FIG. 6. Comparison between the numerical current gradient and the analytic prediction calculated via Eq. (53) for both (a) $\frac{U}{t_0} = 0$ and (b) $\frac{U}{t_0} = 7$ when driven by the $\Phi(t)$ shown in Fig. 4.

Eqs. (14) and (52):

$$
\frac{dJ(t)}{dt} = -2eat_0 \frac{d\Phi(t)}{dt} R(\psi) \cos[\Phi(t) - \theta(\psi)]
$$
$$
- 2eat_0 U C(\psi) \cos[\Phi(t) - \kappa(\psi)], \tag{53}
$$

which provides a valuable consistency check for numerical simulations.

The Ehrenfest theorem also resolves the problem of $\Phi_T(t)$ being only unique modulo 2π when $|\psi\rangle$ is unique. If at time t, $\Phi_T(t)$ correctly reproduces $J_T(t)$, then $\Phi_T(t) \rightarrow \Phi_T(t) + 2n\pi$, $n \in \mathbb{Z}$ will generate the same current. This means that at each time, one in fact has an infinite number of choices for $\Phi_T(t)$. This nonuniqueness leads to $\Phi_T(t)$ being nondifferentiable. To see this, consider

$$
\frac{d\Phi(t)}{dt} = \lim_{\Delta t \rightarrow 0} \frac{\Phi_T(t + \Delta t) - \Phi_T(t)}{\Delta t}. \tag{54}
$$

If the derivative exists for this solution, then the switching solution to (for instance) $\Phi_T(t + \Delta t) \rightarrow \Phi_T(t + \Delta t) + 2n\pi$ would render Φ_T nondifferentiable, as the limit on the right-hand side of Eq. (54) would not exist. For the Ehrenfest theorem to be meaningful, however, $\frac{d\Phi(t)}{dt}$ must exist. For this reason, the additional solutions resulting from adding integer multiples of $2n\pi$ at any time cannot be admitted as physical. Equation (53) uniquely specifies $\frac{d\Phi(t)}{dt}$, and stipulating that the evolution must obey this means that for a given initial condition, $\Phi_T(t)$ has a unique solution. To test the Ehrenfest theorem, we take two systems at $U = 0$ and $U = 7t_0$, and drive them with the $\Phi(t)$ shown in Fig. 4. All results are obtained with a numerically exact time propagation of the correlated state. More details for these reference systems can be found in Ref. [19].

Figure 6 compares the dipole acceleration $\frac{dJ(t)}{dt}$ calculated using Eq. (53) to the numerical gradient. It can be seen that both calculations align perfectly, as they must for the system evolution to be considered physical. Extending this to tracking control, Fig. 7 provides an example demonstrating that the Ehrenfest theorem is obeyed when tracking the current of a different system. This highlights the fact that the theorem is obeyed in two systems with the same current gradient,
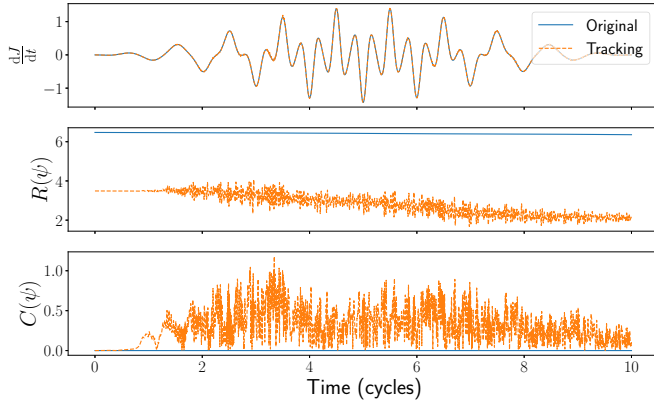
FIG. 7. When tracking the original $J(t)$ from the $U = 0$ system in the $U = 7t_0$ system, we find that $\frac{dJ_T}{dt}$ when calculated via Eq. (53) agrees with the numerical gradient (top panel). This is despite the fact that the untracked expectations $R(\psi)$ and $C(\psi)$ used in Eq. (53) have different trajectories for each of the two simulations.

despite the fact that the nontracked expectations do not match between simulations.

The verification provided by Ehrenfest theorems is particularly useful for tracking in high-$\frac{U}{t_0}$ simulations, when $\theta(\psi)$ exhibits large oscillations. When this angle is calculated numerically, it is given a value between $[-\pi, \pi]$. If on a time-step update this threshold is crossed, a numerical discontinuity is introduced by the assignment $\theta(\psi) = \pm\pi \pm \delta \rightarrow \mp\pi \pm \delta$. The Ehrenfest theorem is sensitive to this artificial discontinuity, and can therefore be used to correct it in both $\theta(\psi)$ and $\Phi_T(t)$. An example of a control field where this correction is necessary is shown in Fig. 8.

V. TRACKING CONTROL IN CONTINUOUS SYSTEMS

The tracking conditions and behaviors derived in the previous sections were obtained under the assumption of a finite-dimensional system. We now examine the consequences for these properties when performing tracking control in a continuous system. To do so, we consider modeling a single active electron in an atomic system, coupled to an electric field $E(t)$. This is described by the Hamiltonian

$$\hat{H}(t) = \frac{1}{2}\hat{p}^2 + V(\hat{x}) - E(t)\hat{x}. \qquad (55)$$

Tracking control in this model has previously been successfully implemented for tracking $\langle x(t)\rangle$ in Ref. [16]. To make
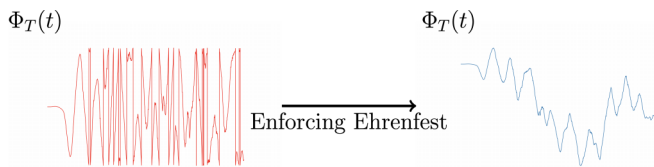
FIG. 8. While $\Phi(t) - \theta(\psi)$ is always constrained to lie between $[-\frac{\pi}{2}, \frac{\pi}{2}]$ modulo 2π, both $\theta(\psi)$ and $\Phi(t)$ can individually undergo large oscillations, which introduce numerical discontinuities. These unphysical discontinuities can be identified by appealing to the Ehrenfest theorem, and removed so as to enforce Eq. (51).

contact with the discrete models considered previously, we apply the Peierls substitution [33]. This amounts to applying a time-dependent unitary transformation $\hat{U}(t) = e^{-iA(t)\hat{x}}$ to obtain an equivalent Hamiltonian in the rotating frame,

$$\hat{H}(t) = \frac{1}{2}e^{-iA(t)\hat{x}}\hat{p}^2 e^{iA(t)\hat{x}} + V(\hat{x}), \qquad (56)$$

where $A(t) = \int_0^t dt' E(t')$ is the vector potential. An appropriate tracking variable in this model is $\langle x(t)\rangle$ or its time derivatives. In order to relate $A(t)$ and the target expectation, one must discretize the model either in time or space. If one takes a spatial discretization, using a lattice $\{x_j\} = \{ja\}$, then one obtains a hoppinglike Hamiltonian,

$$\hat{H} \rightarrow -\frac{1}{2a^2}\sum_j (e^{-iaA(t)}|x_{j+1}\rangle\langle x_j| + e^{iaA(t)}|x_j\rangle\langle x_{j+1}|)$$

$$+ \sum_j \left[V(x_j) + \frac{1}{a^2}\right]|x_j\rangle\langle x_j|. \qquad (57)$$

From this discretization, it is possible to derive a tracking equation for $\langle\frac{dx(t)}{dt}\rangle$,

$$\left\langle\frac{dx(t)}{dt}\right\rangle = -\frac{R_a(\psi)}{2a^2}\sin[aA(t) - \theta_a(\psi)], \qquad (58)$$

where

$$\sum_j \langle\psi|(|x_{j+1}\rangle\langle x_j| - |x_j\rangle\langle x_{j-1}|)|\psi\rangle = R_a(\psi)e^{i\theta_a}. \qquad (59)$$

This tracking equation has precisely the same form as those derived in Sec. II, and the same analyses concerning tracking constraints and nonuniqueness can be applied to tracking $\langle\frac{dx(t)}{dt}\rangle$ with identical results.

If one instead works in the continuum, it is possible to obtain a tracking equation for $\langle x(t)\rangle$ by discretizing time to obtain

$$\langle\hat{x}(t+dt)\rangle = \langle\hat{x}(t)\rangle + \frac{1}{2}dt\left[\left\langle\frac{dx}{dt}(t)\right\rangle + \left\langle\frac{dx}{dt}(t+dt)\right\rangle\right]$$

$$+ \frac{1}{4}dt^2\left[\left\langle\frac{d^2x}{dt^2}(t)\right\rangle + \left\langle\frac{d^2x}{dt^2}(t+dt)\right\rangle\right] + O(dt^3), \qquad (60)$$

where a midpoint rule has been applied to the discretization of the expectation derivatives. Substituting for the expectations $\langle\frac{dx(t)}{dt}\rangle = \langle e^{-iA(t)\hat{x}}\hat{p}e^{iA(t)\hat{x}}\rangle$ and $\langle\frac{d^2x}{dt^2}(t)\rangle = -\langle\partial_x V(\hat{x})\rangle$ yields the tracking equation for a continuous system:

$$A(t+dt) = -2\left[\langle\hat{p}\rangle - \frac{\langle\hat{x}(t+dt)\rangle - \langle\hat{x}(t)\rangle}{dt}\right]$$

$$- A(t) + dt\langle\partial_x V(\hat{x})\rangle + O(dt^2). \qquad (61)$$

This tracking equation reduces to exactly that derived in Ref. [16] if one once again applies the midpoint approximation to express $A(t+dt) - A(t) = \frac{dt}{2}[E(t+dt) + E(t)]$.

While this equation will successfully track the target expectation, its continuum nature means that performing a similar Lipschitz analysis is extremely challenging, if not impossible. Note also that unlike in the spatial discretization, if one includes dissipation in the equation of motion, this will result in an additional term in Eq. (61).

TABLE I. Fit parameters for $\bar{\Phi}_T(t)$ when tracking $U = 0$ in the $U = t_0$ system.

	1	2	3
$\frac{E_j}{E_0}$	0.52	3.1×10^{-2}	4.93×10^{-3}
$\frac{\omega_j}{\omega_0}$	1.00	3.01	4.93
δ_j	0	π	1.3π
$\mu = 4.72T$		$\alpha = 1.12 \times 10^{-2}T^{-2}$	

Unlike in the discrete case, the functional dependence of the tracked expectation on the control field is not explicitly periodic, and the nonuniqueness observed in the previous section as a consequence of this is *also* removed. From this, we may conclude that while the tracking control strategy may be used in continuous systems, the advantage of precise tracking constraints, and the phenomena of nonuniqueness are only manifestly present in a finite-dimensional context. This highlights another subtle difference between finite- and infinite-dimensional representations of quantum phenomena [34], although in practice *any* system we wish to simulate must on some level be restricted to a finite-dimensional approximation.

VI. EXPERIMENTAL FEASIBILITY

Although the material mimicry done in Ref. [19] demonstrates that the tracking strategy is successful *in silico*, there remains a question of the experimental feasibility of generating the laser pulses prescribed by the tracking strategy. Although it is possible to implement a control scheme which reflects experimental constraints [7,8], this in general does not guarantee an exact match with the target. In order to guarantee exact tracking in Ref. [19], neither the intensity nor bandwidth of the driving field was constrained.

As a first test of the experimental feasibility of our method, we examine the effect of fitting the control field obtained from the material mimicry in Ref. [19] to a limited number of D distinct frequencies, ω_j. As targets, we consider the $U = 0$ and $U = 1t_0$ systems driven by the reference Φ, given by

$$\Phi(t) = a\frac{E_0}{\omega_0} \sin^2\left(\frac{\pi t}{T}\right) \sin(\omega_0 t), \qquad (62)$$

where T is the total evolution time, and $\Phi(t)$ shown in Fig. 5. We then generate the tracking field $\Phi_T(t)$ necessary for each system to track the reference spectrum produced by the other system, before fitting this to a model $\bar{\Phi}_T(t)$.

For the $U = t_0$ system tracking the reference current generated by the $U = 0$ system, we fit $\Phi_T(t)$ to the model,

$$\bar{\Phi}_T(t) = \Phi(t) + f_E(t) \sum_{j=1}^{D} \frac{a_T E_j}{\omega_j} \sin(\omega_j t - \delta_j), \qquad (63)$$

where $f_E(t)$ is a two-parameter envelope function given by

$$f_E(t) = e^{-\alpha(t-\mu)^2} \sin^2\left(\frac{\pi t}{T}\right). \qquad (64)$$

Using this model, we are able to obtain a reasonable fit for $\bar{\Phi}_T$ for $D = 3$, with the relevant laser field parameters shown
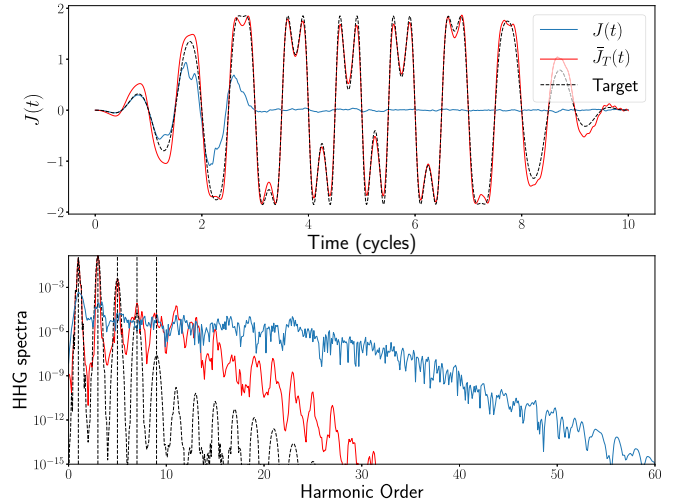
FIG. 9. Tracking current in the $U = t_0$ system. Here, $J(t)$ is the current produced by $\Phi(t)$, while $\bar{J}_T(t)$ is the current produced by the best-fit control field $\bar{\Phi}_T(t)$. The target is the current produced by $\Phi(t)$ in the $U = 0$ system.

in Table I. The results of driving the system with the fitted $\bar{\Phi}_T$ are shown in Fig. 9. We find that the fitted control field tracks the target reasonably well, accurately reproducing the first five harmonics of the target current. When compared to untracked driving with $\Phi(t)$, the performance of $\bar{\Phi}_T$ in reproducing the target current is markedly superior.

When tracking the $U = t_0$ reference current in the $U = 0$ system, the fitted model is amended slightly,

$$\bar{\Phi}_T(t) = f_E(t) \sum_{j=1}^{D} \frac{a_T E_j}{\omega_j} \sin(\omega_j t - \delta_j), \qquad (65)$$

but retains the same functional form for the envelope function. Once again, reasonable fits are obtained for $D = 3$, with parameters given in Table II. Results for the currents generated by this fitting, $\bar{\Phi}_T$, are shown in Fig. 10. When examining the frequency space, the fitted control field does not perform as well when compared to the previous case, but this is to be expected given the broadband nature of the target field. In the time domain (where the control field phases are relevant), we find $\bar{\Phi}(t)$ is still able to capture the most prominent features of the target current, and once again performs markedly better than using the reference $\Phi(t)$.

TABLE II. Fit parameters for $\bar{\Phi}_T(t)$ when tracking $U = t_0$ in the $U = 0$ system.

	1	2	3
$\frac{E_j}{E_0}$	0.89	0.27	4.5×10^{-2}
$\frac{\omega_j}{\omega_0}$	1.07	3.12	3.86
δ_j	0.12π	0.48π	-0.41π
$\mu = 0.6T$		$\alpha = 0.15T^{-2}$	
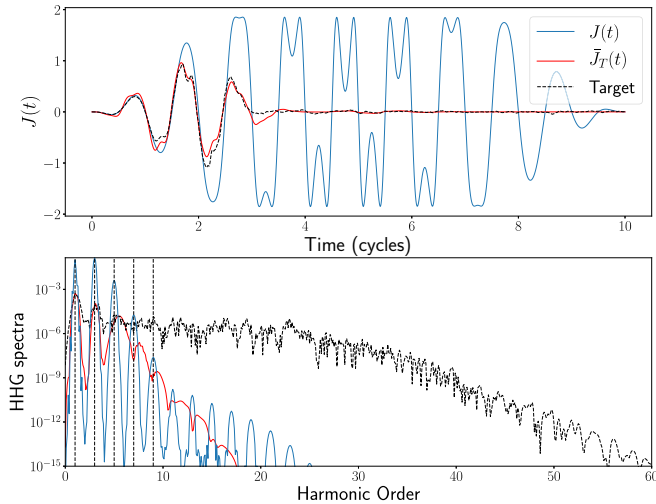
FIG. 10. Tracking current in the $U = 0$ system. Here, $J(t)$ is the current produced by $\Phi(t)$, while $\bar{J}_T(t)$ is the current produced by the best-fit control field $\bar{\Phi}_T(t)$. The target is the current produced by $\Phi(t)$ in the $U = t_0$ system.

VII. DISCUSSION

In this paper, we have expanded on the work presented in Ref. [19]. In addition to providing a more complete derivation for the tracking model's equation of motion, constraints guaranteeing Hermiticity and a unique evolution were rigorously derived. Although these constraints restrict the size of imitable currents in tracking, this can be circumvented either by scaling the current one wishes to track or modifying system parameters such that the constraints are obeyed. The ability to transparently identify and remove singularities via scaling represents a tangible advantage over more generic tracking strategies [14,17,32].

The derived constraints of Eqs. (28) and (29) also highlight an interesting ambiguity in the tracking model, namely, that in some circumstances multiple control fields will track the same target expectation. This raises a question for future investigations about the enumeration of these solutions and how their dynamics differ. An Ehrenfest theorem for the tracked expectation was also introduced for the purpose of verifying the consistency of the numerics with the constraints of physical principles. Insistence that this Ehrenfest theorem be obeyed removes unphysical discontinuities that can arise from the periodic effect of $\Phi(t)$ on the dynamics.

In investigating the potential to realize this tracking experimentally, we found that in the considered cases, reasonable approximations of the target currents could be obtained using, at most, three frequencies in addition to the reference field $\Phi(t)$. This suggests that some form of tracking control is achievable with current technology. Finally, the same concepts used to derive the model presented here could potentially be applied to optimal dynamic discrimination (ODD). This problem is essentially the converse to that of tracking control, in which one distinguishes very similar quantum systems using the dynamics induced by properly shaped laser pulses [35,36]. Given that the requirements for discrimination are similar to those for tracking control, the former may benefit from the techniques presented here.

[1] J. Werschnik and E. K. U. Gross, J. Phys. B **40**, R175 (2007).

[2] I. Serban, J. Werschnik, and E. K. Gross, Phys. Rev. A **71**, 053810 (2005).

[3] P. Doria, T. Calarco, and S. Montangero, Phys. Rev. Lett. **106**, 190501 (2011).

[4] A. P. Peirce, M. A. Dahleh, and H. Rabitz, Phys. Rev. A **37**, 4950 (1988).

[5] C. Winterfeldt, C. Spielmann, and G. Gerber, Rev. Mod. Phys. **80**, 117 (2008).

[6] S. J. Glaser, U. Boscain, T. Calarco, C. P. Koch, W. Köckenberger, R. Kosloff, I. Kuprov, B. Luy, S. Schirmer, T. Schulte-Herbrüggen, D. Sugny, and F. K. Wilhelm, Eur. Phys. J. D **69**, 279 (2015).

[7] D. M. Reich, J. P. Palao, and C. P. Koch, J. Mod. Opt. **61**, 822 (2014).

[8] J. P. Palao, R. Kosloff, and C. P. Koch, Phys. Rev. A **77**, 063412 (2008).

[9] R. Kosloff, A. D. Hammerich, and D. Tannor, Phys. Rev. Lett. **69**, 2172 (1992).

[10] A. Bartana, R. Kosloff, and D. J. Tannor, J. Chem. Phys. **99**, 196 (1993).

[11] G. Katz, M. A. Ratner, and R. Kosloff, Phys. Rev. Lett. **98**, 203006 (2007).

[12] A. Sukhov and J. Berakdar, Phys. Rev. Lett. **102**, 057204 (2009).

[13] A. Rothman, T.-S. Ho, and H. Rabitz, Phys. Rev. A **72**, 023416 (2005).

[14] A. Magann, T.-S. Ho, and H. Rabitz, Phys. Rev. A **98**, 043429 (2018).

[15] T. Caneva, T. Calarco, and S. Montangero, Phys. Rev. A **84**, 022326 (2011).

[16] A. G. Campos, D. I. Bondar, R. Cabrera, and H. A. Rabitz, Phys. Rev. Lett. **118**, 083201 (2017).

[17] W. Zhu and H. Rabitz, J. Chem. Phys. **119**, 3619 (2003).

[18] W. Zhu, M. Smit, and H. Rabitz, J. Chem. Phys. **110**, 1905 (1999).

[19] G. McCaul, C. Orthodoxou, K. Jacobs, G. H. Booth, and D. I. Bondar, Phys. Rev. Lett. **124**, 183201 (2020).

[20] H. Kleinert, *Particles and Quantum Fields* (World Scientific, Singapore, 2016).

[21] H. Tasaki, J. Phys. Condens. Mater. **10**, 4353 (1998).

[22] A. Nocera, A. Polkovnikov, and A. E. Feiguin, Phys. Rev. A **95**, 023601 (2017).

[23] G. B. Folland, *Real Analysis: Modern Techniques and Their Applications* (Wiley, New York, 2007).

[24] R. K. Nagle, *Fundamentals of Differential Equations and Boundary Value Problems*, 6th ed. (*Featured Titles for Differential Equations*) (Pearson, Boston, 2011).

[25] R. Horn, *Matrix Analysis* (Cambridge University Press, Cambridge, 1985).

[26] A. Borzi, G. Ciaramella, and M. Sprengel, *Formulation and Numerical Solution of Quantum Control Problems* (Society for Industrial and Applied Mathematics, Philadelphia, 2017).

[27] E. W. Hobson, Proc. London Math. Soc. **s2-7**, 14 (1909).

[28] A. Jha, V. Beltrani, C. Rosenthal, and H. Rabitz, J. Phys. Chem. A **113**, 7667 (2009).

[29] F. Gebhard, *The Mott Metal-Insulator Transition: Models and Methods* (Springer Tracts in Modern Physics) (Springer, New York, 2010).

[30] F. H. L. Essler, *The One-Dimensional Hubbard Model* (Cambridge University Press, Cambridge, 2005).

[31] In fact, the ground state is potentially highly degenerate depending on the number of sites and filling fraction, but since we are only arguing that the ground-state energy is nonzero, it is sufficient to treat the ground state as a pure state in the occupation number representation.

[32] R. Hirschorn and J. Davis, SIAM J. Control Optim. **25**, 547 (1987).

[33] R. Feynman, *The Feynman Lectures on Physics* (Basic Books, a member of the Perseus Books Group, New York, 2011).

[34] D. I. Bondar, R. Cabrera, and H. A. Rabitz, Phys. Rev. A **88**, 012116 (2013).

[35] B. Li, G. Turinici, V. Ramakrishna, and H. Rabitz, J. Phys. Chem. B **106**, 8125 (2002).

[36] A. Goun, D. I. Bondar, A. O. Er, Z. Quine, and H. A. Rabitz, Sci. Rep. **6**, 25827 (2016).